

Research on Acquisition Method of MBOC/Sideband AltBOC Signals

Deng Zhong-liang*, Yin Lu, Xi Yue, Zhan Zhong-wei, Dong Hui, Wang Guan-yi

Beijing University of Posts and Telecommunications

No.10 Xi Tu Cheng Road, Beijing, 100876

*Corresponding author, e-mail: dengzhl@bupt.edu.cn

Abstract

New GNSS signal systems (MBOC/AltBOC) are different from traditional one (BPSK). Acquisition methods of new signal systems need to be studied to adapt the new modulation scheme. On the other hand, there are more acquisition cells and long stop time on each cell because of the features of the new GNSS signal systems. So the average acquisition time of the new signals increase much longer than the former one. The new signal features was analyzed at first in this paper, and then the acquisition algorithm of QPSK and MBOC modulated signals was introduced separately. At last, a Multiplexing Channel of Time-Division technique and Multi-frequency aid algorithm was proposed to increase the acquisition speed. This new fast acquisition algorithm significantly reduced the average acquisition time of the new GNSS signal systems.

Keywords: acquisition, MBOC, sideband AltBOC, channel multiplexing, multi-frequency aid

Copyright © 2014 Institute of Advanced Engineering and Science. All rights reserved.

1. Introduction

With the development of the new navigation system, such as GPS (Global Positioning System) modernization process and the BeiDou Navigation Satellite System, multi navigation system and the interoperability are the trend of satellite navigation. Multi-system receiver of GNSS (Global Navigation Satellite System) has advantages of good coverage, high positioning accuracy and high reliability. Receivers can get rid of dependence on a single system, and has a better RAIM (Receiver Autonomous Integrity Monitoring) [1].

There are lots of differences of the new GNSS signal systems, such as MBOC, AltBOC and QPSK modulation signals, from the traditional one, such as BPSK modulation of GPS L1 C/A. The signal spectrum is splitted because of the modulation of sub-carrier. This avoids the interference between the new signals and the traditional one. A pilot component is also added to the new signal systems for a better sensitivity. However, The traditional algorithm will cost a longer time to acquire signals because of the longer length or higher frequency of the PRN code [2]. The acquisition method of new signal systems was introduced in this paper first. And then proposed a fast acquisition algorithm by analyzing the features of new signal systems. It is gained a shorter time of processing in the hardware by the Multiplexing Channel of Time-Division, and shorten the time of acquisition by multi-frequency aid method because of the decrease of searching patterns.

2. Acquisition of GNSS Signals

The new GNSS signal systems, such as GPS L1C, GPS L5, Galileo E1 and Galileo E5 signal, has developed rapidly. Those signals modulated with BOC or sideband AltBOC (processed as QPSK modulation [3]) which have a better ranging accuracy and anti-jamming performance. So we can get a better positioning accuracy and reliability by using the new signal systems. Table 1 shows the main parameters of some new signal systems.

As Table 1 shows, GPS L1C and Galileo E1 have a lot in common. First, they have the same carrier frequency, bandwidth and code frequency. Then, CBOC (6,1,1/11) and TMBOC(6,1,4/33) can be classified as CBOC (6,1,1/11) modulation. Similarly for the GPS L5 and Galileo E5a signals have the same conclusion because of sideband AltBOC (15,10) can be

processed as QPSK (10). It can reduce the design complexity of a GNSS receiver because of those commons and have a better performance by using those signal systems [4].

Table 1. Main Parameters of Some New Signal Systems

signal systems	Galileo E1	GPS L1C	Galileo E5a	GPS L5
Carrier frequency (MHz)	1575.42	1575.42	1176.45	1176.45
Bandwidth (MHz)	24.552	24.552	20.46	20.46
Modulation method	CBOC(6,1,1/11)	TMBOC(6,1,4/33)	Sideband AltBOC(15,10)	QPSK
Code frequency (Mchips/s)	1.023	1.023	10.23	10.23
Code length	4092	10230	10230	10230
Code period (ms)	4	10	1	1

Using the carrier-code two-dimensional acquisition method to acquire the GNSS signal as Figure 1 shows [5]. The Doppler range of carrier frequency is -5kHz to 5kHz with the step of f_{bin} . The range of code phase is 0 to M chips with the code length of M and code step of Δ_d . The time-domain parallel search method is used for a shorter acquisition time. There are $N_{Parallel}$ correlators working simultaneously on a Doppler bin to correlate the input signal with local codes of different phases. The correlation results is compared to an acquisition threshold to determine whether acquire the signal in the $N_{Parallel}$ cells.

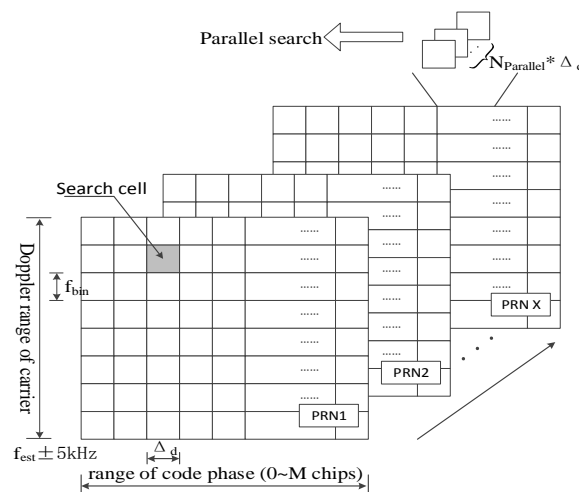


Figure 1. Two-dimensional Acquisition Method

2.1. Sideband AltBOC (QPSK) Signal Acquisition

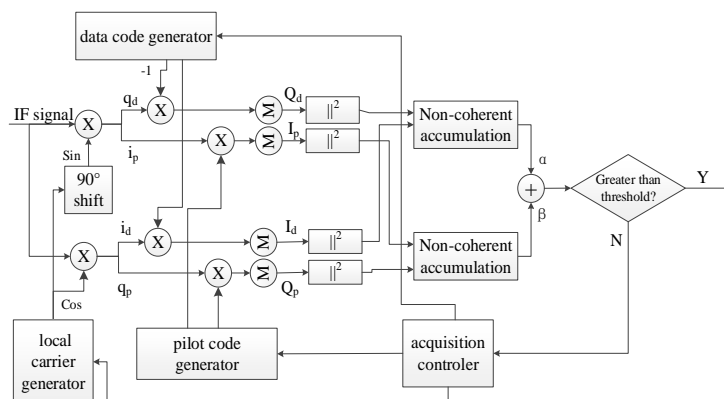


Figure 2. Acquisition Structure of QPSK Signal

Data and pilot component of GPS L5/Galileo E5a signal modulated by QPSK are identified by quadrature carriers and PRN codes. The acquisition structure of QPSK signal is illustrated by Figure 2.

The expression of QPSK IF signal is [6]:

$$s_{QPSK}(t) = \sqrt{P_d} D(t) S e_d(t) C_d(t) \cos[2\pi(f + f_D)t + \varphi] + \sqrt{P_p} S e_p(t) C_p(t) \sin[2\pi(f + f_D)t + \varphi] + n_0 \quad (1)$$

Where d is the data component, p is the pilot component, P is the energy of the signal, D is the data, $S e$ is the second or NH code, C is the PRN code, f is the intermediate frequency, f_D is the Doppler, φ is the phase of input carrier, and n_0 is the noise. Local carrier is:

$$\begin{cases} carr_i(t) = \cos[2\pi(f + f'_D)t + \varphi'] \\ carr_q(t) = \sin[2\pi(f + f'_D)t + \varphi'] \end{cases} \quad (2)$$

Where f'_D is the local Doppler and φ' is the phase of local carrier. The correlation result of in-phase component of data component is as Equation (3) shows without the consideration of flips of data or second code.

$$\begin{aligned} I_d &= \int_0^{T_{coh}} s_{QPSK}(t) carr_i(t) C'_d(t) dt \\ &= \frac{\sqrt{P_d}}{2} T_{coh} R_{Cd}(\tau) \text{sinc}(\Delta f_D T_{coh}) \cos(\pi \Delta f_D T_{coh} + \Delta \varphi) + n_{0,Id} \end{aligned} \quad (3)$$

Where T_{coh} is the coherent integration time, C' is the local code, Δf_D is the Doppler difference of local and input carriers, $\Delta \varphi$ is the phase difference of local and input carriers, R_{Cd} is the autocorrelation function of PRN code of data component, R_{Cd-p} is the cross-correlation function of PRN codes of data and pilot component, τ is the phase difference of local and input codes, and $n_{0,Id}$ is the equivalent noise. Similarly:

$$Q_d = \frac{\sqrt{P_d}}{2} T_{coh} R_{Cd}(\tau) \text{sinc}(\Delta f_D T_{coh}) \sin(\pi \Delta f_D T_{coh} + \Delta \varphi) + n_{0,Qd} \quad (4)$$

$$I_p = \frac{\sqrt{P_p}}{2} T_{coh} R_{Cp}(\tau) \text{sinc}(\Delta f_D T_{coh}) \cos(\pi \Delta f_D T_{coh} + \Delta \varphi) + n_{0,Ip} \quad (5)$$

$$Q_p = \frac{\sqrt{P_p}}{2} T_{coh} R_{Cp}(\tau) \text{sinc}(\Delta f_D T_{coh}) \sin(\pi \Delta f_D T_{coh} + \Delta \varphi) + n_{0,Qp} \quad (6)$$

Where R_{Cp} is the autocorrelation function of PRN code of pilot component. Squaring and summing I and Q components for the correlation envelope:

$$\begin{aligned} V &= \sqrt{(I_d^2 + Q_d^2) + (I_p^2 + Q_p^2)} \\ &= \frac{\sqrt{P_{QPSK}}}{2} T_{coh} R_C(\tau) |\text{sinc}(\Delta f_D T_{coh})| + n_p \end{aligned} \quad (7)$$

Where V is the correlation envelope, $P_{QPSK} = P_d + P_p$ is the energy of signal, and n_p is the equivalent noise. Because V will decrease with the increase of Δf_D , f_{bin} is approximated by Equation (8):

$$f_{bin} = \max(\Delta f_D) = \frac{2}{3T_{coh}} \tag{8}$$

f_{bin} is 667Hz with T_{coh} of GPS L5/Galileo E5a signal is 1ms. The autocorrelation function of PRN code is as Figure 3 shows when $f_{bin}=500\text{Hz}$. $\Delta_d=0.5$ chips is appropriate from Figure 3.

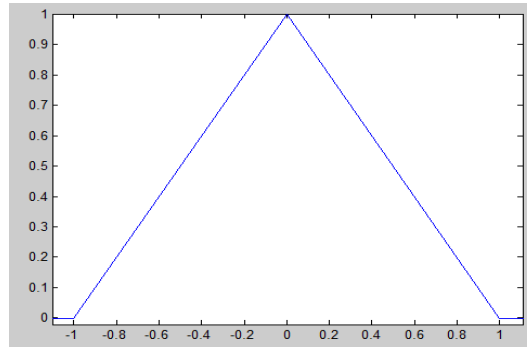


Figure 3. Autocorrelation Function of PRN Code (GPS L5/Galileo E5a signal)

2.2. MBOC Signal Acquisition

Data and pilot component of GPS L1C/Galileo E1 signal modulated by MBOC are identified by PRN codes. An equivalent code combined with PRN code and sub-carrier is needed for correlating the MBOC signal. The acquisition structure of MBOC signal is illustrated by Figure 4.

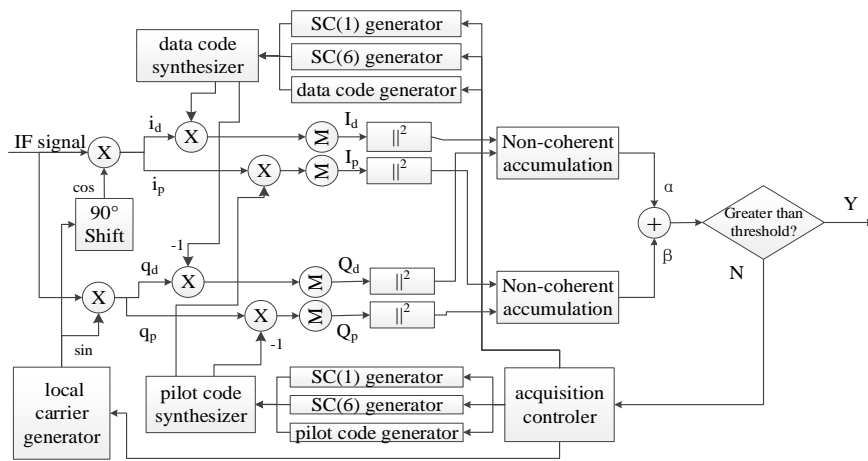


Figure 4. Acquisition Structure of MBOC Signal

The expression of MBOC IF signal is [7]:

$$s_{MBOC}(t) = \left[\sqrt{P_d} D(t) C_d(t) S_{c_d}(t) + \sqrt{P_p} S_e(t) C_p(t) S_{c_p}(t) \right] \cos[2\pi(f + f_D)t + \varphi] + n_0 \tag{9}$$

$$= \left[\sqrt{P_d} D(t) \hat{C}_d(t) + \sqrt{P_p} S_e(t) \hat{C}_p(t) \right] \cos[2\pi(f + f_D)t + \varphi] + n_0$$

Where Sc is the sub-carrier and $\hat{C}(t)$ is the equivalent code. We can get the correlation envelope after correlating input signal with local equivalent code:

$$V = \frac{\sqrt{P_{MBOC}}}{2} T_{coh} R_{\hat{C}}(\tau) |\text{sinc}(\Delta f_D T_{coh})| + n_p \tag{10}$$

Where $R_{\hat{C}}$ is the autocorrelation function of the equivalent code. f_{bin} of E1 and L1C is approximated by Equation (11):

$$\begin{cases} f_{bin,E1} = \frac{2}{3T_{coh,E1}} = 167 Hz = 150 Hz^{Use} \\ f_{bin,L1C} = \frac{2}{3T_{coh,L1C}} = 67 Hz = 50 Hz^{Use} \end{cases} \tag{11}$$

There are multiple peaks of the autocorrelation function of the equivalent code of MBOC signal, which is different from the autocorrelation function of the PRN code of sideband AltBOC (QPSK) signal as Figure 5 shows (the autocorrelation function of the equivalent code of E1 signal is illustrated as Figure 5, and the autocorrelation function of the equivalent code of L1C signal is not illustrated because it is almost the same as the one of E1 signal). The multiple peaks are caused by the sub-carriers modulated on the PRN code. The tow side peaks are caused by SC(1) which narrows the main peak at the same time. The irregular shape of the autocorrelation function is caused by SC(6).

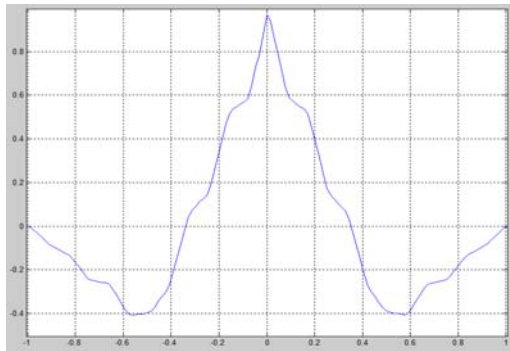


Figure 5. Autocorrelation Function of the Equivalent Code (MBOC signal)

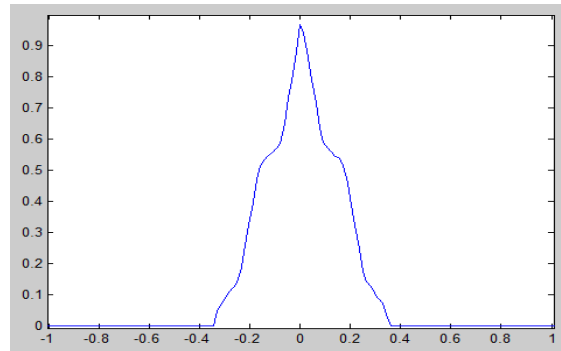


Figure 6. Autocorrelation Function of the Equivalent Code of MBOC Signal Without Side Peaks

The side peaks must be eliminated because it might cause the bycatch at the wrong code phases. Using Equation (12) to eliminate the side peaks with the consideration of the flip of the data bit [8]:

$$\hat{R}_{\hat{C}}(\tau) = \frac{R_{\hat{C}}(\tau) + D(t) |R_{\hat{C}}(\tau)|}{2} \tag{12}$$

The new autocorrelation function of the equivalent code of MBOC signal is illustrated as Figure 6 ($D(t) > 0$). The main peak is narrower and steeper than the autocorrelation function of the PRN code of sideband AltBOC (QPSK) signal. So the Δ_d is appropriated to 0.25.

2.3. Dual-component Combined Acquisition

Both data and pilot components are broadcasted in new signal systems of GNSS. The navigation messages which are needed in the PVT (Position, Velocity and Time) solution are modulated on the data component while the NH codes or secondary codes which are known are modulated on the pilot component. A higher sensitivity is gained by a longer coherent integration of the pilot component in tracking because of the known secondary codes. Either data or pilot component can be used in acquisition judgement. But there will be some energy loss in single component acquisition. The ratio of data and pilot components energy is 1:3 of GPS L1C signal while 1:1 of GPS L5, Galileo E1 and E5a signals. So there will be 1.25dB~6.0dB energy loss for the above signals in single component acquisition. It will lead to leak detect when the signal is weak. So the dual-component combined acquisition is needed for a maximum energy. The single data component acquisition and dual-component combined acquisition results of GPS L5 are shown as Figure 7(a) and (b). The maximum energy of single data component acquisition is only near 6000 while above 8000 in dual-component combined acquisition. So there is a higher sensitivity when use dual-component combined acquisition.

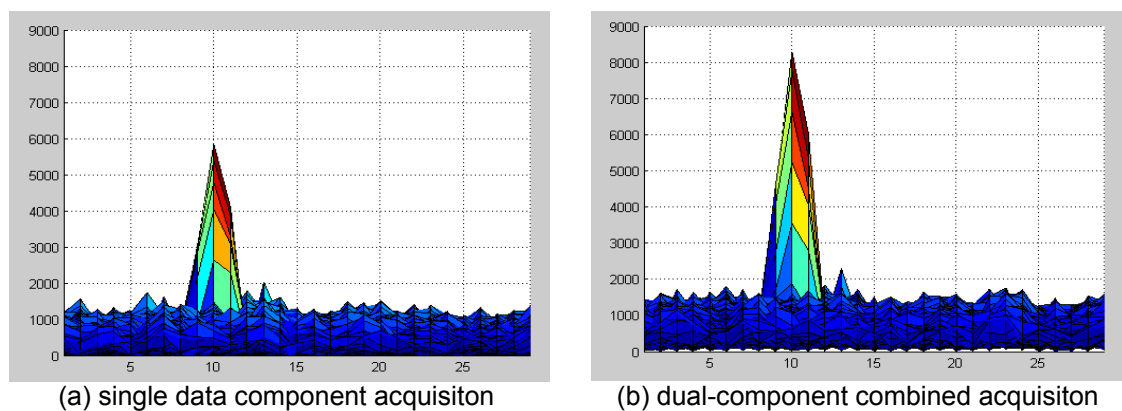


Figure 7. Acquisition Results of GPS L5

2.4. Threshold of Acquisition

Correlation envelope is calculated as Equation (7) or Equation (10). Assuming that the noises yield Gaussian distributions with mean of zero and variance of σ_n^2 . The correlation envelope yields Rayleigh distribution when the signal not exist while yields the Ricean distribution when the signal exist as Figure 8 shows.

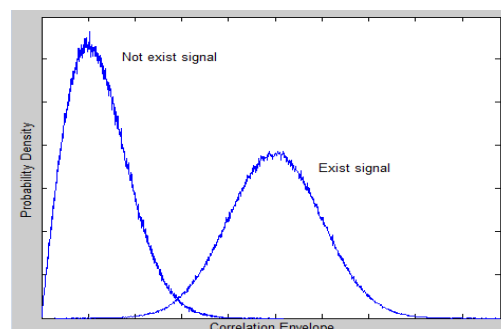


Figure 8. The Distribution of the Correlation Envelope

The acquisition threshold is calculated as Equation (13) shows with coherent integration only:

$$V_t = \sigma_n \sqrt{-2 \ln P_{fa}} \quad (13)$$

Where σ_n^2 is the power of noise, P_{fa} is the probability of false alarm. We can get the threshold by measuring the received noise with a specific probability of false alarm. There is $\sigma_n^2 = \frac{1}{2K} \sum_{n=1}^K (I^2(n) + Q^2(n))$ when the signal not exist (simulated by a coherent integration using a invalid PRN code quadratured with other valid PRN codes). Where K is the times of caculating. σ_n^2 will converge to the true value with the increasing of K.

2.5. Acquisition Efficiency

The average acquisition time is one of the important items that reflects the acquisition capability and is given by [9]:

$$T_{acq} = \frac{1}{2} \frac{N_{cell}}{N_{Parallel}} T_{dwell} \quad (14)$$

Where T_{dwell} is the stop time on each cell, and N_{cell} is total amount of acquisition cells which is given by:

$$N_{cell} = \left(\frac{2 * 5kHz}{f_{bin}} + 1 \right) \frac{M}{\Delta d} \quad (15)$$

The average acquisition time of the new signal systems (L5, E5a, L1C, and E1) is much longer than the one of the old signal system (L1 C/A) as Table 2 shows. Multiplexing channel of time-division and multi-frequency aid methods proposed by this paper are the way to shorten acquisition time.

Table 2. The Average Acquisition Time of Some GNSS Signals

Signal system	Frequency (MHz)	f_{bin} (Hz)	M (chip)	Δ_d (chip)	T_{dwell} (s)	$N_{Parallel}$	T_{acq} (s)
L1 C/A	1575.42	500	1023	0.5	0.001	128	0.17
L5	1176.45	500	10230	0.5	0.001	128	1.68
E5a	1176.45	500	10230	0.5	0.001	128	1.68
L1C	1575.42	50	10230	0.25	0.01	128	321.3
E1	1575.42	150	4096	0.25	0.004	128	17.32

3. Multiplexing Channel of Time-Division

The local signal correlates with input signal driven by the sampling clock. The correlator outputs an integration result every code period and it is idle in most of processing progress because of the much lower sampling clock than the maximum processing clock of FPGA or ASIC. The Multiplexing Channel of Time-Division technique proposed by this paper multiple the sampling clock by N to get a high processing clock. Then the N correlators correlate the N local signals of different phases with the input signal one processing clock after another.

The timing diagram of the Multiplexing Channel of Time-Division technique is illustrated as Figure 9. Take GPS L1 C/A signal for example, $sample_clk$ is the sampling clock of 62MHz, $code_clk$ is the code generation clock of 1.023MHz, and $code[0]$ - $code[6]$ are the 1/2 PRN codes of N (N=7 here) different phases of satellite 1 (1101010 for the first 7 chips) as Figure 9(a) shows. Enlarge the first half-chips as Figure 9(b) shows. Where $high_clk$ is the processing clock (7 * sampling clock here), and data is the input signal sampled by $sample_clk$. N bits PRN code with different phases (1111001 here) is generated clocked by $high_clk$ in a $sample_clk$ period. Then correlate the input data with the N bits code one $high_clk$ after another to get N correlation results. The average acquisition time decrease N times by the Multiplexing Channel of Time-Division technique.

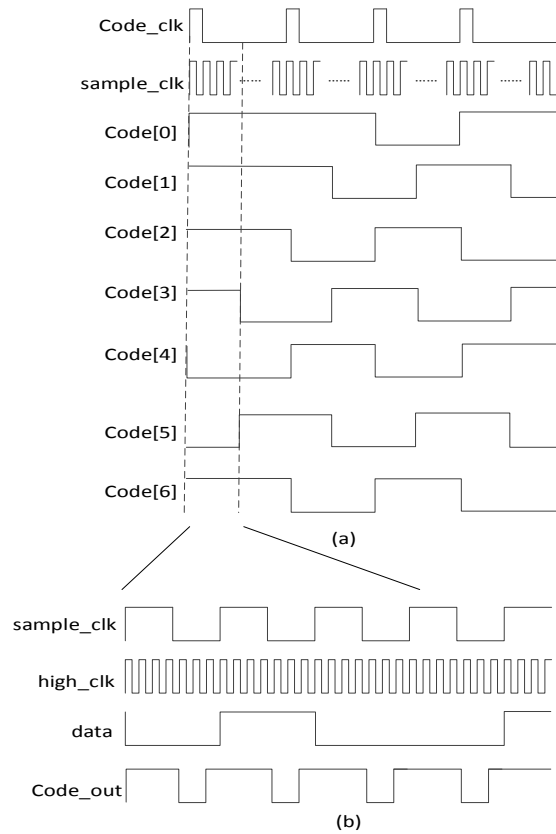


Figure 9. Timing Diagram of the Multiplexing Channel of Time-Division Technique

4. Multi-frequency Aid

MBOC signals are aided by QPSK signals because of its small f_{bin} , Δ_d and long T_{dwell} . We acquire the QPSK signal first and then use its Doppler and code phase to aid the acquisition of MBOC signal. Multi-frequency aid include the Doppler aid and the code phase aid.

4.1. Doppler Aid

The Doppler of carrier frequency is given by [10]:

$$f_D = \frac{v}{c} f_{car} \quad (16)$$

Where v is the relative velocity between the antenna and satellite, c is the speed of light and f_{car} is the carrier frequency. The Doppler of L5 frequency ($f_{D,L5}$) is known when acquired the satellite and the Doppler of L1 frequency ($f_{D,L1}$) will be calculated as Equation (15):

$$f_{D,L1} = \frac{f_{L1}}{f_{L5}} f_{D,L5} \quad (17)$$

There is an ambiguity of 250Hz from the acquisition of QPSK signal because of $f_{bin,QPSK}=500\text{Hz}$. The Doppler ambiguity might be up to (250 ± 500) Hz when acquired the signal at the adjacent frequency bin in the condition of low C/N0. It needs a more accurate Doppler because the range of (250 ± 500) Hz is too wide for L1C signal ($f_{bin,L1C}=50\text{Hz}$). The Doppler ambiguity will be below 10Hz when the signal is tracked. And then it becomes a one-dimensional (code phase dimensional) acquisition rather than two-dimensional because of the little Doppler ambiguity. So the average acquisition time decreases $10\text{kHz}/f_{bin}$ times by Doppler aid.

4.2. Code Phase Aid

We can get a very accuracy code phase because the code frequency of QPSK signal is ten times higher than the one of MBOC signal. But there is a code phase integer ambiguity of $M \cdot 1023$ ($M_{E1}=4$, $M_{L1C}=10$) because of the lower code length of QPSK signal as Figure 10 shows. So the code phases on the M integer ambiguity is needed to acquire and the average acquisition time decrease $1023/M$ times by code phase aid.

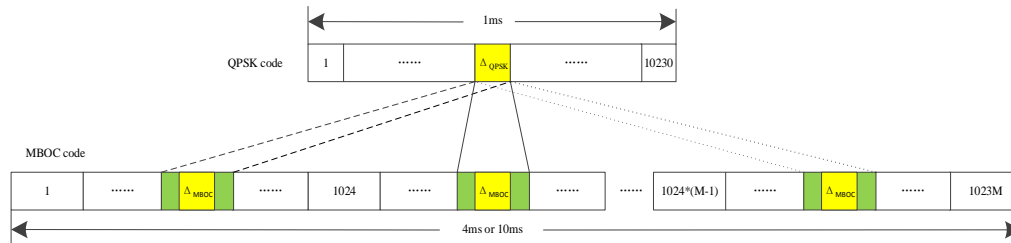


Figure 10. Code Phase Aid Schematic

4. Conclusion

An acquisition method is introduced in this paper by analyzing the features of new signal systems. Then proposed a fast acquisition algorithm for GNSS multi-system interoperability signals for a short acquisition time. The parallelism of the acquisition cells is improved by the Multiplexing Channel of Time-Division technique. Then the acquisition cells of MBOC signal are reduced by the aid of the Doppler and code phase of QPSK signal. The average acquisition time decrease $(N \cdot 10\text{kHz} \cdot 1023 / f_{\text{bin}} / M)$ times for E1 and L1C signals, and N times for E5a and L5 signals by the algorithm proposed in this paper.

References

- [1] Li CX, Chun HL. Study on the MBOC signal common-used by GPS and Galileo. *GNSS World of China*. 2009; 34(4): 47-51.
- [2] Yang L, Pan CS, Feng YX. A New Algorithm for Synchronous Main Lobe Detection for BOC Modulated Navigation Signals. *Journal of Astronautics*. 2012; 38(8): 2008-2014.
- [3] Zhang ZY, Zhang LX, Meng YS. Study of acquisition technology for AltBOC signal. *Modern Electronics Technique*. 2012; 35(5): 55-59.
- [4] Li JW, Li ZH, Hao JM. A Preliminary Study on Compatibility and Interoperability of GNSS. *Journal of Geomatics Science and Technology*. 2009; 26(3): 177-180.
- [5] Kaplan ED, Hegarty CJ. *Editors. Understanding GPS-Principles and Applications (Second Edition)*. Boston: Artech House Publications. 2006.
- [6] Li XQ, Luo XZ, Li J. A New Way to Deduce Power Spectrum of AltBOC Modulation Signal. *Radio Engineering*. 2012; 42: 34-64.
- [7] Zhu XF, Chen XY. Performance analysis of MBOC modulation in next generation GNSS. *Journal of Chinese Inertial Technology*. 2009; 18(4): 434-438.
- [8] Zhou YL, Hu XL, Tang ZP. *Unambiguous tracking technique for Sin-BOC(1,1) and MBOC(6,1,1/11) signals*. 2010 2nd International Conference on Future Computer and Communication. Wuhan. 2010; 1: 1188-1190.
- [9] Hao Y, Liu XF, Gu XM. A Low-Cost PN code acquisition scheme. *Journal of Harbin Institute of Technology*. 2005; 37(4): 515-517.
- [10] Bao J, Tsui Y. *Editors. Fundamentals of global positioning system receivers: a software approach*. Hoboken: John Wiley & Sons Publications. 2005.